Wang *et al. Nutrition & Metabolism* (2025) 22:47
https://doi.org/10.1186/s12986-025-00938-9

Nutrition & Metabolism

RESEARCH Open Access

Multi-omics analysis reveals *Lactobacillus* and Indolelactic acid involved in small intestinal adaptation of piglet with short bowel syndrome

Weipeng Wang[1†], Ying Lu[2,3,4†], Bo Wu[2], Shicheng Peng[3,4], Wei Cai[1,2,3,4] and Yongtao Xiao[1,2,3,4*]

Abstract

Background Short bowel syndrome (SBS) is a condition characterized by malabsorption that occurs when a patient loses a significant amount of bowel length or function, often necessitating lifelong parenteral nutrition support. This study utilized multi-omics analysis to investigate alterations in gut microbiota, metabolism, and transcriptome during the progression of intestinal adaptation in SBS using a piglet model.

Methods We established a model of SBS in Bama mini piglets by performing a 75% jejunoileal resection. Fifteen piglets were randomized into EN, PN, and PN-SBS groups. Fecal samples were collected for 16 S rRNA gene-based microbiota analysis. Ileal mucosa and serum were collected for untargeted liquid chromatography-mass spectrometry. Transcriptomic analysis on ileal mucosa was performed.

Results The PN-SBS model was established in the newborn piglets. A significant decrease in species-level diversity was observed in piglets with SBS, accompanied by alterations in their microbiome compositions. The beneficial anaerobes from *Bacillota* and *Bacteroidota* were depleted while microorganisms from *Verrucomicrobiota* and *Fusobacteriota* were enriched in feces from SBS piglets. The dysregulation of metabolites and metabolic pathways was observed in the metabolic profiles of ileal mucosa and serum in SBS piglets. Indolelactic acid (ILA) levels were found to be reduced in the ileal mucosa and serum of SBS piglets. Transcriptomic analysis revealed an extensive functional alteration in SBS, primarily manifested as metabolic changes and intestinal proliferation. The multi-omics analysis revealed that the decreased abundance of *Lactobacillus* may result in a diminished production of their metabolite ILA, thereby influencing intestinal proliferation and anti-inflammatory responses.

Conclusion Disrupted homeostasis of gut microbiota, metabolism, and transcriptome were reported in the SBS piglets. Multi-omics analysis demonstrated *Lactobacillus* and its metabolite ILA may be involved in small intestinal adaptation of SBS. These alterations may contribute to the proinflammatory state and the delay of intestinal adaptation in SBS, which in turn provide promising targets for therapies.

[†]Weipeng Wang and Ying Lu are contribute to this work equally.

*Correspondence:
Yongtao Xiao
xiaoyongtao@xinhuamed.com.cn

Full list of author information is available at the end of the article

Keywords Short bowel syndrome, Multi-omics, Microbiome, Metabolomics

Introduction

Short Bowel Syndrome (SBS) is a condition characterized by malabsorption, stemming from congenital defects, substantial surgical resection of the small intestine, or disease-induced loss of absorptive capacity [1, 2]. It stands as the primary cause of intestinal failure among children and accounts for 50% of cases requiring home parenteral nutrition [3]. SBS poses a significant threat to patients' lives and quality of life, as the remaining intestinal tissue often fails to sustain adequate nutritional balance for proteins, fluids, electrolytes, and micronutrients without additional support from parenteral or enteral nutrition [4]. The prognosis of SBS highly depends on several factors, including the extent of intestinal resection, the patient's age and overall health, and the effectiveness of intestinal adaptation [5]. Intestinal adaptation involves a series of morphological, functional, and metabolic changes [6]. Morphologically, the remaining intestine undergoes hypertrophy, with an increase in the villus height and crypt depth, leading to an expansion of the absorptive surface area. Functionally, the intestine enhances its absorptive capacity by increasing the expression and activity of nutrient transporters and digestive enzymes [5, 7]. The gut microbiota plays a crucial role in maintaining gastrointestinal health and function. In SBS, the altered anatomy and physiology of the gastrointestinal tract can lead to significant disruptions in the gut microbiota composition [8]. Previous studies have shown that SBS patients often exhibit dysbiosis, characterized by a reduction in microbial diversity and an overrepresentation of potentially pathogenic bacteria [8]. This dysbiosis can contribute to increased intestinal permeability, inflammation, and impaired nutrient absorption, further exacerbating the clinical manifestations of SBS [9]. Metabolically, patients with SBS often experience alterations in their energy metabolism, with increased reliance on alternative energy sources such as fat and protein catabolism [5]. Recent study has identified distinct metabolic profiles in SBS patients, highlighting the importance of specific metabolites in gut health and disease [10]. For instance, alterations in bile acid metabolism, amino acid profiles, and short-chain fatty acids (SCFAs) have been reported in SBS patients. These changes reflect the complex interplay between the gut microbiota, host metabolism, and nutritional status. Thus, providing a clear understanding of the pathogenic basis of intestinal adaptation on SBS is critical for the treatment and healthcare of this complex disease.

The progression of intestinal adaptation on SBS encompasses changes at the genetic, transcriptional, proteomic, and metabolic levels [11]. Thus, by integrating multi-omics technologies such as genomics, transcriptomics, proteomics, and metabolomics, a more comprehensive understanding of the biological mechanisms underlying the progression of intestinal adaptation can be achieved. Additionally, multi-omics analysis aids in the discovery of new biomarkers and therapeutic targets related to SBS. In this study, we established an SBS model using the Bama mini piglets and conducted a comprehensive multi-omics analysis to elucidate the intricate interactions among gut microbiota, metabolism, and transcriptome.

Materials and methods

Animal experiments and sample collection

Seven-day-old Guangxi Bama minipigs (0.8–1 kg) were purchased from Jiagan Biotechnology (Shanghai, China) and housed in a light-controlled room with a 12 h light/dark cycle at the Experimental Animal Center of Xinhua Hospital. All animal research protocols were reviewed and approved by the Experimental Animal Care and Use Committee of Xinhua Hospital Affiliated to Shanghai Jiao Tong University School of Medicine (XHEC-F-2020-008).

Fifteen Bama Mini-piglets were randomly divided into the EN group ($n=5$), PN group ($n=5$), and PN-SBS group ($n=5$). The procedure of PN and the PN formulation follow the method we previously reported [12, 13]. The piglets underwent SBS operations after an 8-hour fasting period. Prior to the operation, anesthesia was induced with an intramuscular injection of Zoletil-50 (25 mg/kg, Virbac, France), and maintained with Isoflurane (Abbott Laboratories). Afterward, 75% of jejunoileal resection was conducted in the PN-SBS group as described [14]. The small bowel was first measured from the ligament of Treitz to the ileocecal valve. A distal 75% resection was performed and the remaining intestine was joined through a single layer, hand-sewn, end-to-end jejunoileal anastomosis. Postoperatively, analgesia with carprofen injection was provided for 72 h. All animals received ampicillin before the surgical incision. Postoperatively, animals received daily intramuscular injections of ampicillin (50 mg/kg body weight) for 72 h. The piglets were housed individually in separate cages to ensure accurate monitoring and individualized care. Energy intake and composition of macronutrients of the EN groups were identical as described previously [13].

All piglets were sacrificed after 14 days of surgery (Supplemental Fig. 1A-B). The small bowel was remeasured from the ligament of Treitz to the ileocecal valve. The samples were collected for further analysis, including feces, serum, ileum, colon, colonic contents, etc.

Intestinal morphometrics

Different intestinal segments were fixed in 10% buffered formalin and stained with H&E-staining. The histological scores of the ileum were determined based on the extent of villous atrophy, fusion, and inflammatory infiltration, as described previously [15]. The scoring ranges from 0 to 3 as follows: 0 = no pathological or morphological changes; 1 = mild villous atrophy, fusion, and mild inflammatory infiltration; 2 = moderate villous atrophy and fusion with moderate inflammatory infiltration; 3 = severe villous atrophy and fusion with severe inflammatory infiltration. All histological measurements were performed by experienced pathologists who were blinded to the groups.

Microbiota analysis

16 S rRNA sequencing and bioinformatics analysis were performed as we previously described [12, 13]. In brief, fecal samples were collected into sterile containers, subsequently frozen in liquid nitrogen, and kept at a temperature of -80 °C for storage. DNA extraction was carried out using the DNeasy PowerSoil Kit (manufactured by QIAGEN, Inc., Netherlands), following the manufacturer's guidelines. The V4-V5 segment of the bacterial 16 S rRNA gene was amplified with the forward primer 515 F (sequence: 5′- GTGCCAGCMGCCGCGGTAA-3′) and the reverse primer 907R (sequence: 5′-CCGTCAATTCMTTTRAGTTT-3′). The resulting PCR products were purified using Agencourt AMPure Beads (supplied by Beckman Coulter, Indianapolis, IN, USA), and their concentrations were determined using the PicoGreen dsDNA Assay Kit (from Invitrogen, Carlsbad, CA, USA). Following individual quantification, the amplicons were combined in equal proportions and subjected to paired-end sequencing with a read length of 2 × 300 bp on an Illumina MiSeq platform, utilizing the MiSeq Reagent Kit v3, at Shanghai Personal Biotechnology Co., Ltd (Shanghai, China). The sequence data were processed using Quantitative Insights into Microbial Ecology (QIIME, version 1.8.0) and R packages (version 3.5.0). Low-quality sequences were filtered out and the remaining high-quality sequences were then grouped into operational taxonomic units (OTUs) based on 97% sequence similarity using UCLUST, with the representative sequences matched against the Greengenes Database 10. We employed the Bray-Curtis dissimilarity index to assess beta-diversity and used Principal Coordinates Analysis (PCoA) or Non-metric Multidimensional Scaling (NMDS) to visualize differences in beta-diversity between samples. Partial least squares discrimination analysis (PLS-DA) was applied to show the classification of different groups.

Metabolomics analysis

Ultra-Performance Liquid Chromatography-triple quadrupole mass spectrometry (UPLC-TQMS)-based metabolomics analysis was conducted using the Q300 79 Metabolite Assay Kit (Human Metabolomics Institute, Inc., Shenzhen, Guangdong, China) based on the method previously published with minor modifications [16, 17]. Samples of blood and ileum were collected from three groups of piglets: EN ($n = 5$), PN ($n = 5$), and PN-SBS ($n = 5$). All measurements were conducted using the Waters ACQUITY ultra-performance LC system paired with a Waters XEVO TQ-S mass spectrometer featuring an ESI source, controlled by MassLynx 4.1 software (Waters, Milford, MA). Chromatographic separations took place on an ACQUITY BEH C18 column (1.7 μm, 100 mm × 2.1 mm) from the same manufacturer. The system operated in both positive (POS) and negative (NEG) ion modes. The raw data from the UPLC-TQMS were processed using TMBQ software (v1.0, HMI, Shenzhen, Guangdong, China), which facilitated peak integration, calibration, and quantification of each metabolite. The TMBQ software, licensed under GNU GPL V3 and implemented in Java and R, is freely accessible at http://119.136.25.134:9011. Following this, orthogonal partial least-squares-discriminant analysis (OPLS-DA) and univariate tests were employed to detect differences among groups using the IP4M platform [17]. Metabolites with a univariate test p-value less than 0.05 were deemed statistically significant. We utilized the Human Metabolome Database (HMDB) and the KEGG (Kyoto Encyclopedia of Genes and Genomes) database for pathway enrichment analysis, leveraging the hsa (Human Serum Albumin) library for metabolite identification and annotation. The pathway enrichment analysis was conducted using the hypergeometric test to identify significantly enriched pathways based on the metabolite profiles.

Transcriptome (mRNA) sequencing and data analysis

The ileal epithelia were obtained through scraping at 4 °C. Total RNA was extracted with the RNeasy mini kit (Qiagen, Germany). Paired-end libraries were synthesized using the TruSeq® RNA Sample Preparation Kit (Illumina, United States) following the TruSeq® RNA Sample Preparation Guide. In brief, the poly-A-containing mRNA molecules were purified using poly-T oligo-attached magnetic beads. Following purification, the mRNA was fragmented into small pieces using divalent cations under 94 °C for 8 min. The cleaved RNA fragments were copied into first-strand cDNA using reverse transcriptase and random primers. This process was followed by second-strand cDNA synthesis using DNA Polymerase I and RNase H. These cDNA fragments underwent an end repair process, the addition of a single "A" base, and ligation of the adapters. The products were

purified and enriched with PCR to create the final cDNA library. Purified libraries were quantified by a Qubit® 2.0 Fluorometer (Life Technologies, United States) and validated by an Agilent 2100 Bioanalyzer (Agilent Technologies, United States) to confirm the insert size and calculate the mole concentration. Cluster ($n = 3$) was generated by cBot with the library diluted to 10 pM and then was sequenced on the Illumina HiSeq 2500 (Illumina, United States; read length: 150 bp and sequencing depth: 6G) at Shanghai Biotechnology Corporation. Raw reads were preprocessed with Seqtk to filter out sequencing adapters, short-fragment reads and other low-quality reads. Then, Hisat2 v2.0.4 was used to map the cleaned reads to the Rnor 6.0.95 reference genome with two mismatches. After genome mapping, Cufflinks v2.1.1 was run with a reference annotation to generate FPKM values for known gene models. Differentially expressed genes were identified using Cuffdiff v2.2.1. The p-value significance threshold in multiple tests was set by the false discovery rate (FDR). The fold-changes were also estimated according to the FPKM in each sample. The differentially expressed genes were selected using the following filter criteria: p-value $\leqq 0.05$ and fold-change $\geqq 2$. The differentially expressed genes were analyzed for gene set enrichment analysis (GSEA) with the KEGG databases.

Multi-omics analysis

To assess the relationships between different omics datasets, we performed matrix correlation analysis using the Spearman rank correlation coefficient. Given the heterogeneous nature of the datasets (compositional vs. quantitative), we applied appropriate transformations to ensure comparability and compatibility for correlation analysis. For microbiota data, the relative abundance data were transformed using the log-ratio transformation (logCPM) to handle the compositional nature of microbiota data. This transformation stabilizes variances and mitigates the effects of sparsity and zero values. For metabolite data, metabolite concentrations were log-transformed (log2) to normalize the distribution and stabilize variances, which is a standard practice for metabolomics data. For transcriptomic data, gene expression data were normalized using the Transcripts Per Million (TPM) method, followed by log2 transformation to ensure a normal distribution and comparability with other datasets. The Spearman rank correlation matrices were computed between the transformed datasets to identify significant associations. The resulting correlation matrices were visualized using heatmaps, with color scales representing the strength and direction of the correlations.

Statistical analysis

The data were presented as mean ± SEM or median ± interquartile range (IQR), depending on the indication. GraphPad Prism 8.0 (GraphPad Software Inc., San Diego, CA, USA) was utilized for statistical analysis and plot creation. Two-tailed Student's t-tests or Mann–Whitney U test were conducted for comparisons between two groups and ordinary one-way ANOVA analysis or the Kruskal-Wallis test was employed for comparisons involving more than two groups. The gut microbiota composition and diversity were analyzed using ordinary one-way ANOVA analysis with Bonferroni's correction. The differential abundance analysis was conducted using the Kruskal-Wallis test, with post hoc pairwise comparisons adjusted using Dunn's correction for multiple comparisons. Statistical significance was determined when $p < 0.05$. We reported the p-values for the two-group analyses and applied adjusted p-values to account for multiple testing.

Results

Altered microbial community structure and composition in SBS

Histologically, compared to the PN group, the PN-SBS group exhibited intestinal injury in the ileum, characterized by severe blunting and shortening of villi, infiltration of mucosal inflammatory cells, and crypt hypoplasia (Supplementary Fig. 1C). Using 16 S rRNA sequencing, the number of operational taxonomic units (OTUs) identified for the EN, PN, and PN-SBS groups were 1673, 1899, and 1377, respectively. A total of 655 OTUs were common to all three groups, as illustrated in the Venn diagram presented (Fig. 1A). To assess microbial diversity in the intestine, alpha diversity analysis of a single sample was conducted using the Shannon index. Compared with the PN group, a significantly decreased microbial richness and α-diversity were found in the SBS group (Fig. 1B). The principal component analysis (PCA) of the microbiota composition in fecal indicated that the gut microbiota was different in PN-SBS piglets compared with the PN group (Fig. 1C). Regarding community similarity, principal coordinate analysis (PCoA) and nonmetric multidimensional scaling (NMDS) demonstrated that a significant impact on the overall microbial composition was found in the SBS group compared to the EN and PN group (Fig. 1D and E). The partial least squares discriminant analysis (PLS-DA) revealed that PN-SBS piglets were distinctly categorized from both EN and PN piglets, suggesting alterations in the gut microbiota profile of the PN-SBS piglets (Fig. 1F).

The histograms depicting the relative abundance indicated variations in the proportions of various bacteria within the three groups of piglets across different taxonomic hierarchies, ranging from phylum to genus (Fig. 2A-D). At the phylum level, a decrease was observed in the abundance of *Bacteroidota* and *Bacillota* in the SBS piglets, while an increase in the abundance of

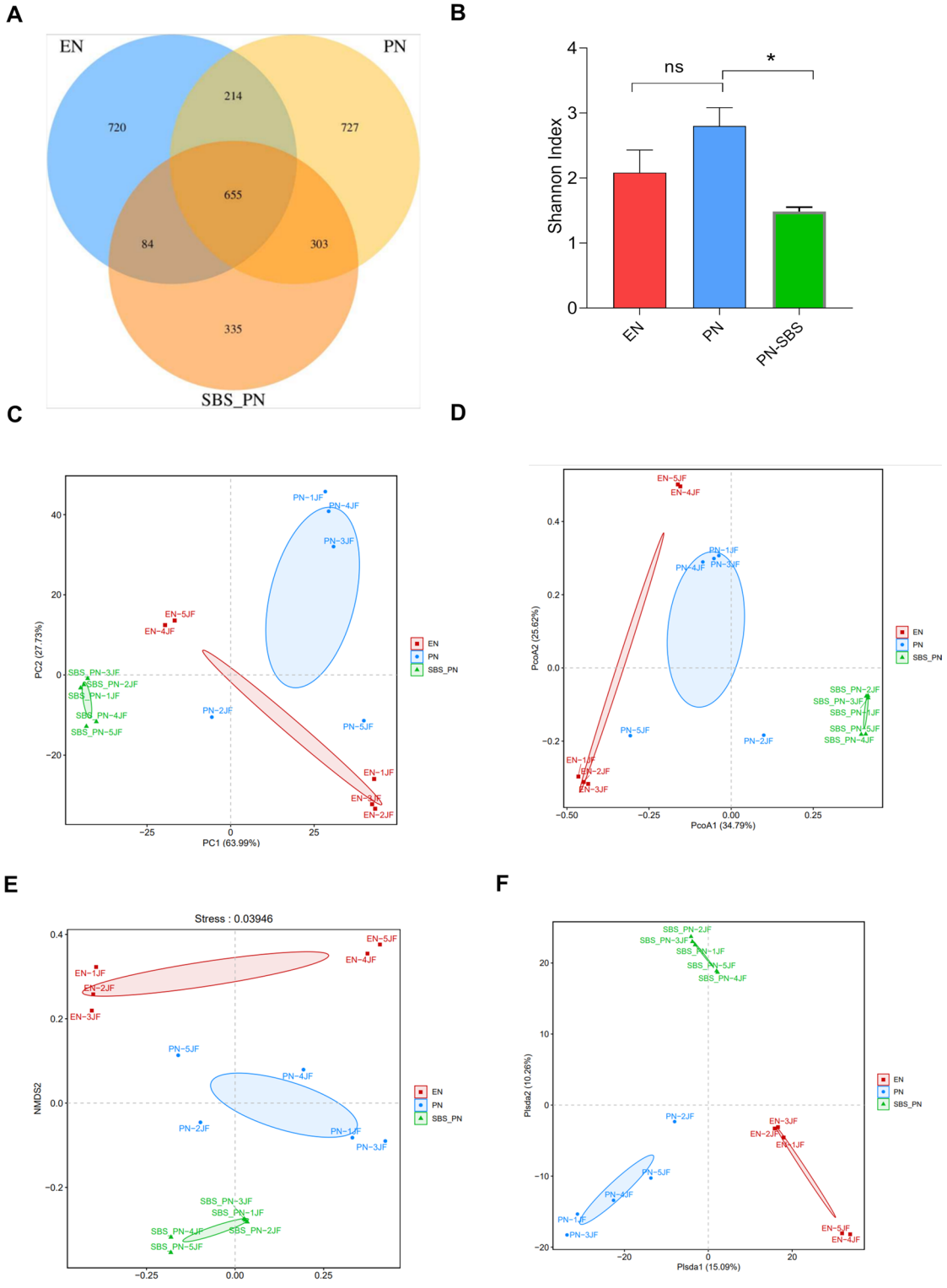

Fig. 1 Gut microbial diversity was modulated in SBS **A**. Venn diagrams showed the differentially operational taxonomic units among the groups of piglets. **B**. Differences in gut microbiota diversity among the groups of piglets were estimated by the Shannon indices. **C**. Principal component analysis plot of 16 S sequencing results derived from feces of the indicated three groups. **D**. Principal coordinate analysis revealed differential community structure among the groups of piglets in the beta diversity analysis. **E**. Nonmetric multidimensional scaling analysis of the gut bacteria data among the groups of piglets. **F**. Partial least square-discriminant analysis showed the changes in gut microbiota diversity among the groups of piglets. Statistical method was used ordinary one-way ANOVA analysis with Bonferroni's correction. Statistical significance: n.s., not significant, $*p < 0.05$, $**p < 0.01$

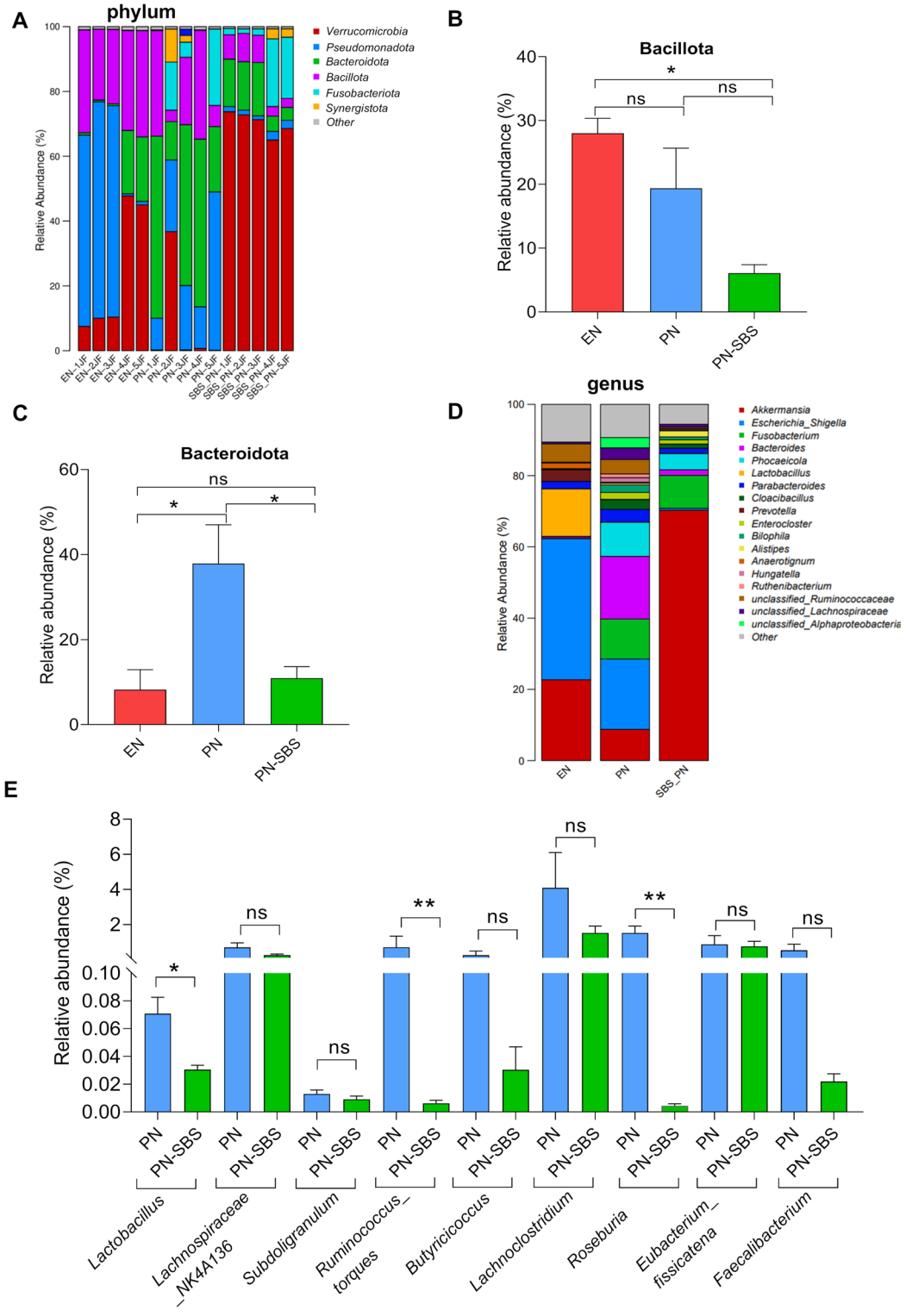

Fig. 2 Gut microbial structure was modulated in SBS. The relative abundance of bacteria was compared at the phylum levels. Comparison of the relative abundance of *Bacillota* among the groups of piglets. Comparison of the relative abundance of *Bacteroidota* among the groups of piglets. The relative abundance of bacteria was compared at the genus levels. Comparison of the relative abundance of genus-level bacteria within the *Bacillota* phylum between the PN and PN-SBS groups of piglets. Statistical method was used Kruskal-Wallis test with post hoc pairwise comparisons adjusted using Dunn's correction for multiple comparisons (B), ordinary one-way ANOVA analysis with Bonferroni's correction (C), the unpaired two-tailed Student's t-test or Mann–Whitney U test (E). Statistical significance: n.s., not significant, $*p < 0.05$, $**p < 0.01$

Verrucomicrobiota and *Fusobacteriota* (Fig. 2A-C). At the genus level, we observed a marked increase in the abundance of bacteria belonging to the *Bacillota* phylum, particularly *Lactobacillus*, *Ruminococcus_torques*, and *Roseburia*, in the SBS group relative to the PN group (Fig. 2D and E).

Dysregulation of metabolites and metabolism pathways in SBS

Metabolomic analysis of ileum and serum was conducted to investigate the metabolic disparities between the PN group and the PN-SBS group. In the ileum, we identified 192 metabolites, including 39 amino acids, 8 SCFAs, 17 carbohydrates, 23 bile acids, 19 carnitines, 24 organic acids, 40 fatty acids, and 22 others (Supplementary Fig. 2A). The relative abundance of indole was decreased in the PN-SBS group compared to the PN group (Fig. 3A and Supplementary Fig. 2B). The orthogonal partial least squares discriminant analysis (OPLS-DA) model clearly distinguished the differential metabolites between the two groups (Fig. 3B). The volcano plot illustrated that 6 differential metabolites were significantly upregulated and 16 differential metabolites were significantly downregulated in the PN-SBS group compared with the PN group (Fig. 3C). As shown in Fig. 3D, the SBS group exhibited reduced levels of certain metabolites, such as indolelactic acid (ILA), glutaric acid, alpha-aminobutyric acid, aspartic acid, etc., while also showing increased levels of other metabolites, including alpha-hydroxyisobutyric acid, ribonic acid, xylose, gluconolactone, etc. Pathway enrichment analysis showed that pathways involved in histidine metabolism, arginine biosynthesis, pentose, and glucuronate interconversions, alanine-aspartate and glutamate metabolism, and Porphyrin metabolism ranked top (Fig. 3E).

In serum, we identified 187 metabolites, including 40 amino acids, 9 SCFAs, 5 peptides, 15 carbohydrates, 13 bile acids, 19 carnitines, 27 organic acids, 40 fatty acids, 4 phenylpropanoic acids, and 15 others (Supplementary Fig. 2A). I The relative abundance of indole was decreased in the PN-SBS group compared to the PN group (Fig. 4A and Supplementary Fig. 2B). The OPLS-DA model showed a distinct separation of the differential metabolites between the two groups (Fig. 4B). As shown in the volcano, there were 10 up-regulated and 27 down-regulated metabolites in the PN-SBS group compared to the PN group (Fig. 4C). As shown in Fig. 4D, the SBS group exhibited reduced levels of certain metabolites, such as ILA, carnosine, citrullin, succinic acid, etc., while also showing increased levels of other metabolites, including butyric acid, isobutyric acid, aspartic acid, methyglutaric acid, etc. Pathway enrichment analysis showed that pathways involved in valine-leucine and isoleucine biosynthesis, alanine-aspartate and glutamate metabolism, arginine biosynthesis, butanoate metabolism, and histidine metabolism ranked top (Fig. 4E).

Alteration in the transcriptomic profiles of SBS ileum

The gut microbiota can manipulate the expression of thousands of genes in intestinal epithelial cells, and thus control intestinal homeostasis and inflammation. To explore the SBS-induced changes in gene expression, ileal mucosa was collected, and the total mRNA was extracted. After reverse transcription, the cDNA was sequenced. The expression of 1781 genes were found to be significantly changed ($p < 0.05$ and fold-change $\geqq 2$) in the PN-SBS group compared to the PN group (Fig. 5A). Among these genes, 160 were downregulated and 1621 were upregulated in the PN-SBS group compared to the PN group (Fig. 5A and B). The top 20 enriched KEGG pathways also showed that SBS might have an impact on intestinal processes of metabolic pathways, and cell proliferation-related pathways (PI3K-AKT signaling pathway, MAPK signaling pathway, and cell cycle) (Fig. 5C). All these results indicate that SBS can the extensive functional changes in the ileum of SBS piglets, with metabolic alterations and intestinal proliferation being the primary manifestations.

The multi-omics analysis in SBS

We conducted a correlation analysis to evaluate the changes in metabolites present in both ileum and serum, in relation to the abundance of bacteria belonging to the *Bacillota* phylum. The abundance of *Lactobacillus* exhibited a significant positive correlation with the metabolites in the ileum, including ILA, aspartic acid, and glutamic acid, whereas the opposite effect with alpha-hydroxyisobutyric acid and gluconolactone (Fig. 6A). Additionally, the abundance of *Lactobacillus* was found to have a significant positive correlation with the metabolites in the serum, including ILA, citrullin, and alanine, whereas the opposite effect with butyric acid and methyglutaric acid (Fig. 6B). We found that ILA was a shared characteristic in the metabolomes of both ileum and serum related to the abundance of *Lactobacillus* (Supplemental Fig. 3A). Moreover, the positive correlation between gut and serum ILA concentrations was found (Supplemental Fig. 3B). The abundance of *Lactobacillus* was positively related to the serum level of citrullin, suggesting an important role of *Lactobacillus* in the intestinal adaption of SBS (Supplemental Fig. 3C). Upon conducting a combined analysis of 16 S rRNA sequencing and transcriptomics, a positive correlation was observed between the abundance of *Lactobacillus* and the expression levels of YAP, IL-22, as well as genes involved in the PI3K-AKT-related signaling pathway, including genes such as CREB3L4, G6PC3, CCND2, and FGF18, among others (Fig. 6C). Furthermore, after performing an

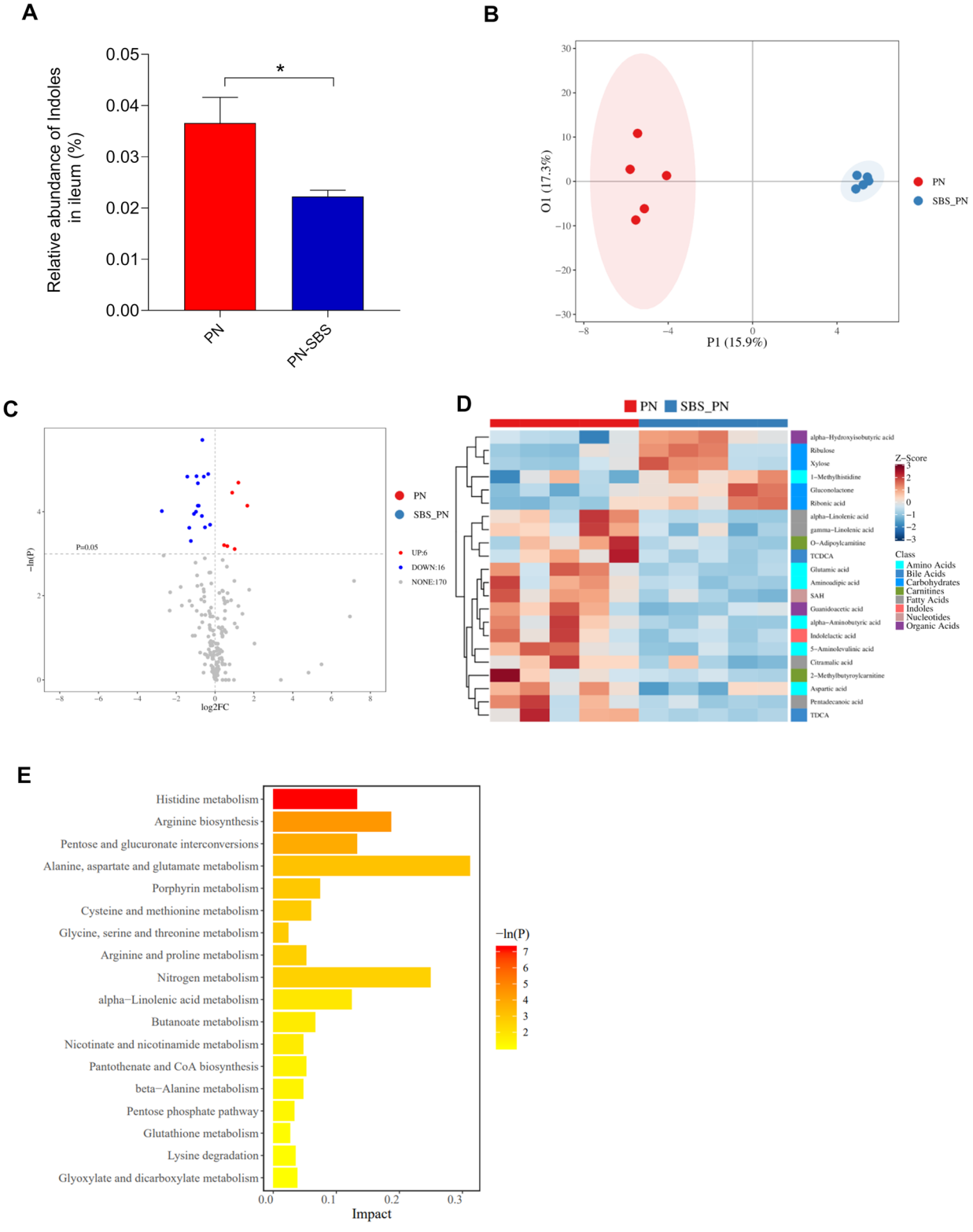

Fig. 3 Differential metabolic patterns perturbed in the ileum of SBS. Comparison of the relative abundance of indoles in the ileum between the PN and PN-SBS group. The orthogonal partial least squares discriminant analysis score plots of ileal metabolites. The volcano plots displayed the statistical significance (P value) versus the magnitude of change (Log2 fold change). Features with Wilcoxon test p value < 0.05 and absolute Log2 fold change > 1 were deemed to be significantly different. The heatmap showed the differently expressed metabolites in the ileum of piglets. Pathway enrichment analysis on differentially expressed metabolites using pathway-associated metabolite sets. Statistical method was used the unpaired two-tailed Student's t-test, Statistical significance: $*p < 0.05$

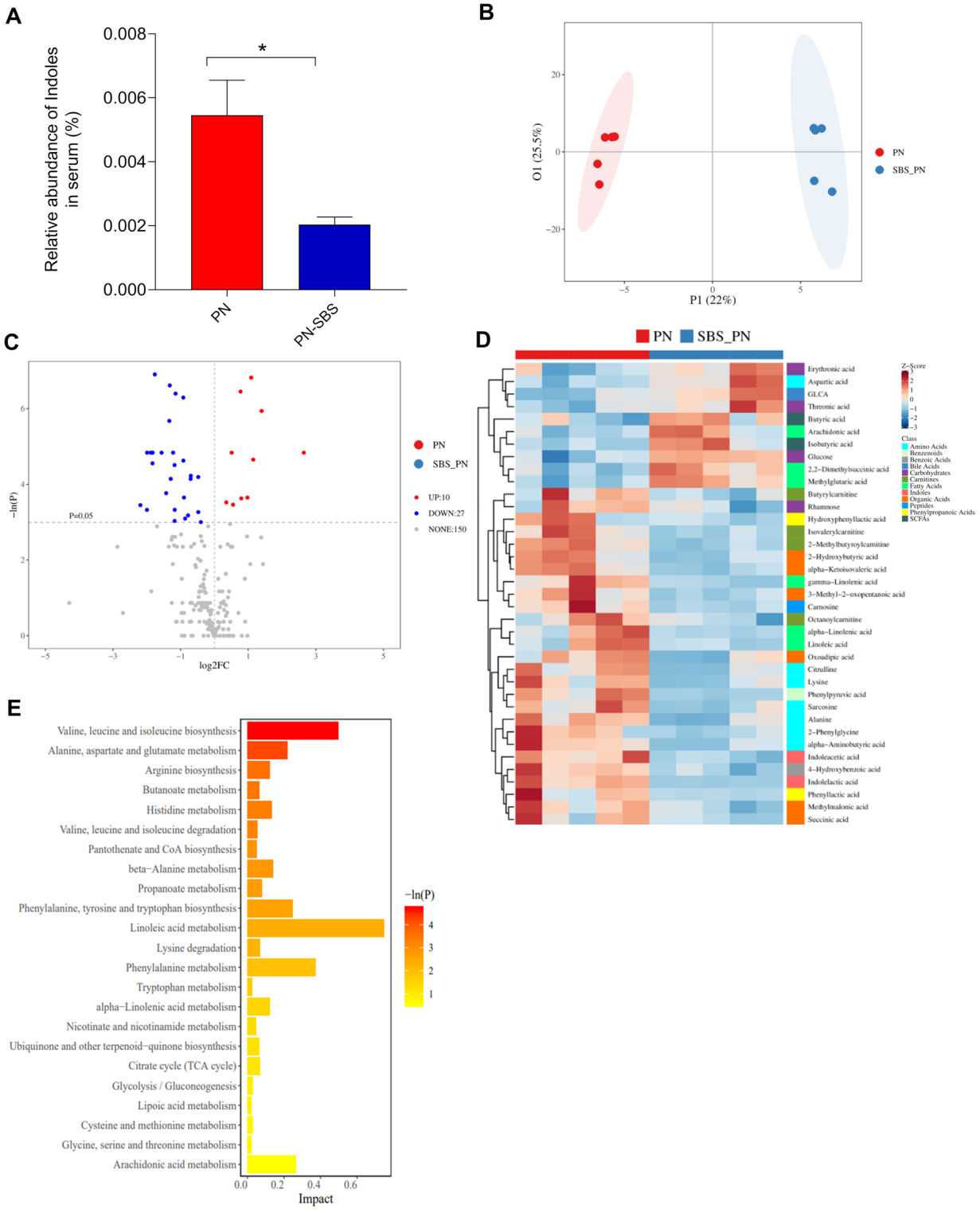

Fig. 4 Differential metabolic patterns perturbed in the serum of SBS. Comparison of the relative abundance of indoles in the serum between the PN and PN-SBS group. The orthogonal partial least squares discriminant analysis score plots of serum metabolites. The volcano plots displayed the statistical significance (P value) versus the magnitude of change (Log2 fold change) in the serum. Features with Wilcoxon test p value < 0.05 and absolute Log2 fold change > 1 were deemed to be significantly different. The heatmap showed the differently expressed metabolites in the serum of piglets. Pathway enrichment analysis on differentially expressed metabolites of serum using pathway-associated metabolite sets. Statistical method was used the unpaired two-tailed Student's t-test, Statistical significance: $*p < 0.05$

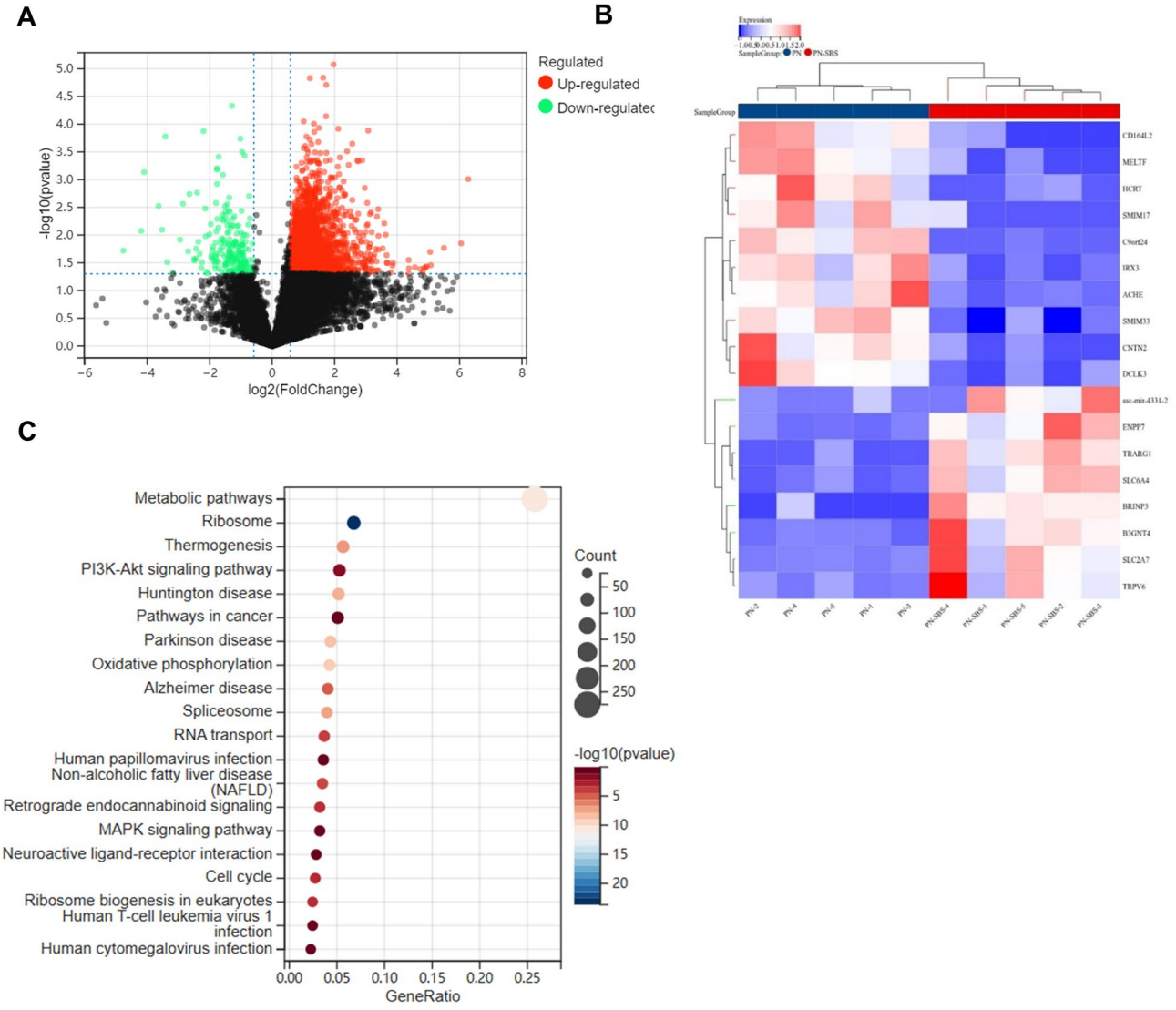

Fig. 5 The altered gene expression profile in SBS. Volcano plots of differentially expressed genes in the ileal mucosa of the piglets between PN and PN-SBS groups. The heatmap showed the differentially expressed genes in the ileum of piglets between PN and PN-SBS groups. KEGG classification of differentially expressed genes between PN and PN-SBS groups and top 20 enriched pathways

integrated analysis combining metabolomics with transcriptomic profiles, we found a significant positive correlation between the presence of *Lactobacillus* and the expression levels of YAP, IL-22, alongside several genes implicated in the PI3K-AKT signaling cascade, notably including CREB3L4, G6PC3, PGF, and CCND2, among various others (Fig. 6D and E). The above results suggest that *Lactobacillus* may promote intestinal adaptation by converting tryptophan into ILA through its metabolic pathway, which in turn enhances the expression of YAP, IL-22, and genes associated with the PI3K-AKT signaling pathway.

Discussion

Advancements in technology within the domains of high-throughput sequencing, metabolomics, and the integration of bioinformatics facilitate a deeper comprehension of the molecular mechanisms involved in the onset and progression of diseases [18]. In this study, we identified the alternation in gut microbes, transcripts, and metabolites using the multi-omics analysis in the piglets for the first time. Notably, the multi-omics analysis suggested a decrease in the abundance of *Lactobacillus* and their metabolite ILA, which may play an essential role in the process of intestinal adaptation. These results are conducive to enhancing our understanding of the underlying molecular mechanisms of SBS.

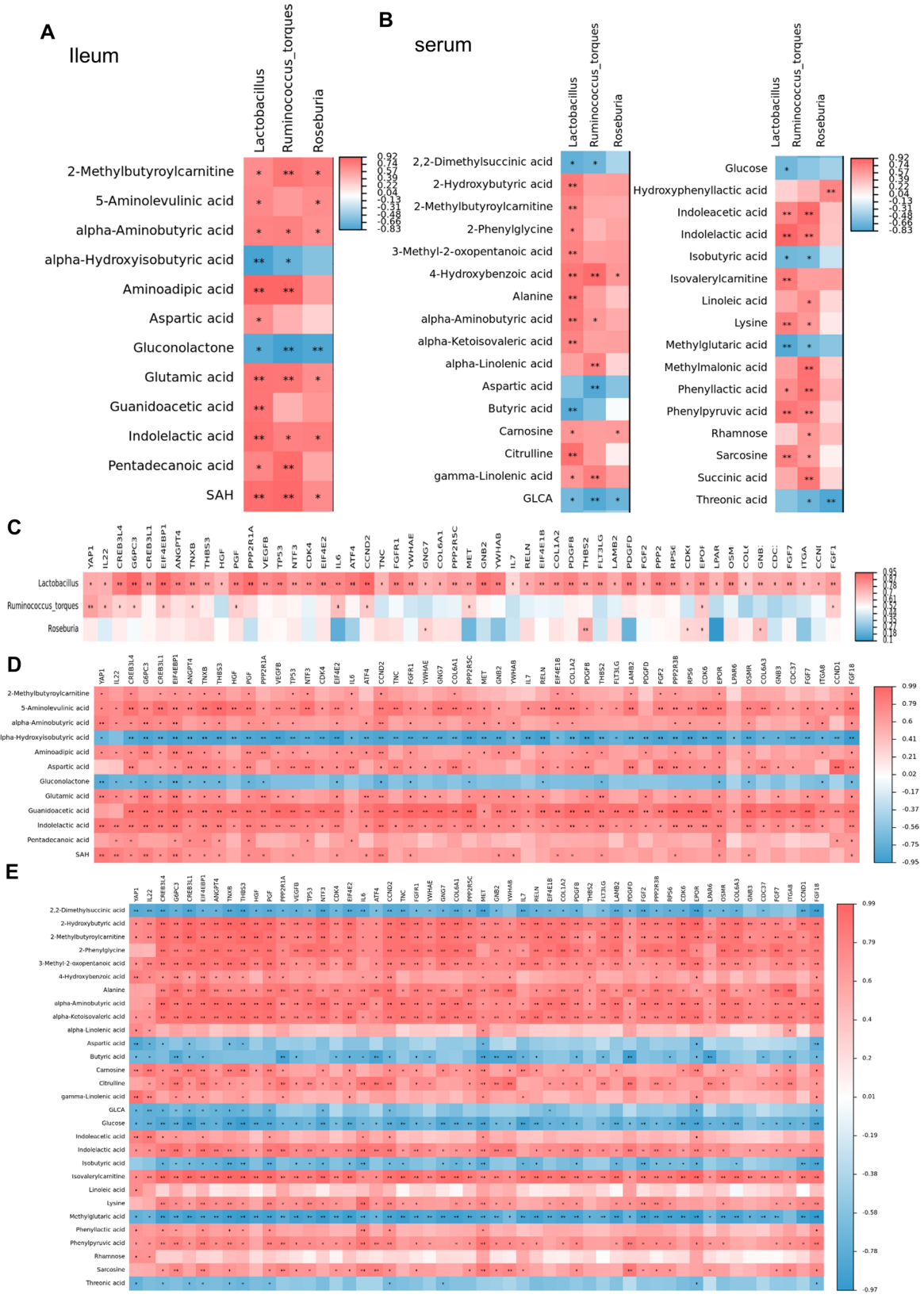

Fig. 6 (See legend on next page.)

(See figure on previous page.)

Fig. 6 Multi-omics analysis revealed the role of *Lactobacillus* and its metabolite ILA in the intestinal adaptation of SBS. Heatmap of Spearman's rank correlation coefficients between differentially abundant species and differential metabolites of ileum from PN and PN-SBS piglets. Heatmap of Spearman's rank correlation coefficients between differentially abundant species and differential metabolites of serum from PN and PN-SBS piglets. Heatmap of Spearman's rank correlation coefficients between differentially abundant species and differentially expressed genes of ileal mucosa from PN and PN-SBS piglets. Heatmap of Spearman's rank correlation coefficients between differential metabolites of ileum and differentially expressed genes of ileal mucosa from PN and PN-SBS piglets. Heatmap of Spearman's rank correlation coefficients between differential metabolites of serum and differentially expressed genes of ileal mucosa from PN and PN-SBS piglets. Statistical method was used the Spearman's rank correlation coefficients, Statistical significance: $*p < 0.05$, $**p < 0.01$

The intestinal tract harbors a vast and diverse microbial community essential for maintaining intestinal homeostasis [19]. Patients with short bowel syndrome have significant changes to their intestinal microbiota after intestinal loss [20]. SBS intestinal bacteria and their metabolites have unique characteristics, which may be the result of pathophysiological changes related to the primary disease (such as Crohn's disease, etc.), or self-adaptive changes after intestinal resection [9]. Conversely, these intestinal bacteria and their metabolites can also act on the remaining intestine and affect intestinal adaptation. Evidence to date suggests significant differences in the microbiome between children with SBS with healthy controls [21]. These differences involve reduced gut microbial diversity, an increase of bacteria associated with inflammation such as *Pseudomonadota*, especially *Enterobacteriaceae*, and a decrease in beneficial bacteria like *Bacteroidot* [21]. Consistent with these observations, we found a reduced gut microbial richness and diversity in the SBS piglets. Previous study has shown a decreased *Bacillota* in SBS rats compared to Sham controls [9]. Consistently, we noted that the down-regulated species characterizing in piglets with SBS mainly belonged to commensal genera within the phylum *Bacillota*, such as *Lactobacillus*, *Clostridium*, *Ruminococcus*, and *Lachnoclostridium*, which can ferment carbohydrates and produce short-chain fatty acids (SCFAs). Numerous studies have confirmed the benefits of *Lactobacillus* as part of the commensal gut flora, including preventing the colonization and translocation of pathogens, restoring gut barrier integrity, and maintaining microbial balance [22–24].

The gut microbiota plays a pivotal role in maintaining overall health by producing metabolites that can influence systemic inflammation, metabolic regulation, and even mental health [25]. The OPLS-DA models revealing remarkably distinct metabolic profiles in SBS relative to PN piglets. We found ILA was a shared characteristic of both the ileum metabolome and the serum metabolome. ILA was severely reduced in the ileal mucosa and serum of SBS piglets compared to control, and its levels correlate with the abundance of Lactobacillus. Huang also observed a reduction in the levels of indole and its derivatives in the feces of rats with SBS [9]. ILA was identified as a key molecule produced by *Lactobacillus* in protecting against intestinal inflammation and correcting microbial dysbiosis [26, 27]. Specifically, Lactobacillus converts tryptophan into ILA, which subsequently enhances the expression of crucial bacterial enzymes involved in tryptophan metabolism, leading to the synthesis of other indole derivatives including indole-3-propionic acid (IPA) and indole-3-acetic acid (IAA) [26]. Previous literature has reported a notable correlation between the abundance of Lactobacillus and ILA levels in mice [22, 26]. Interestingly, our correlation analysis further confirmed the strong positive correlations between ILA and *Lactobacillus* in the piglets, which is the most important ILA producers and decreased in SBS as expected. Additionally, the positive correlation between gut and serum ILA concentrations further supports its relevance as a systemic indicator of gut health. Given that the ILA levels of ileum and serum reductions were concomitant with a decrease of Lactobacillus in SBS, our results may suggest a reduced production of ILA by gut microbiota in the SBS piglets, and the further research is needed to fully elucidate the underlying mechanisms.

ILA is often used as an aryl hydrocarbon receptor (AhR) ligand to regulate innate and adaptive immunity, cell proliferation, inflammation, and apoptosis. ILA has garnered significant attention for its potential role in modulating intestinal health, particularly in intestinal inflammation and intestinal proliferation [28, 29]. ILA can activate the AhR to modulate immune responses of human CD4 + T cells and monocytes, leading to the production of the anti-inflammatory cytokine IL-22 [30]. ILA could protect gut epithelial cells in culture by activating the AhR and Nrf2 pathways [31]. Moreover, studies suggest that ILA plays a beneficial role in maintaining gut barrier integrity, which is crucial for preventing the leakage of harmful substances from the intestine into the bloodstream- a phenomenon that exacerbates inflammation in colitis [22]. Through RNA sequencing, we found that the differentially expressed genes between SBS and PN piglets are mainly enriched in signaling pathways related to metabolism, cell cycle, and other related processes. Further joint analysis of metabolomics and transcriptomics has uncovered a significant positive correlation between the levels of ILA and expressions of IL22. A recent study found ILA promoted the self-renewal of ISCs and protected epithelial cells from inflammation and oxidative stress by regulating YAP and Nrf2 during intestinal ischemia/reperfusion injury [32]. Our study also uncovered a significant positive

correlation between the levels of ILA and expressions of YAP. Moreover, a notable correlation was found between the levels of ILA and genes related to PI3K-AKT signaling pathways. Collectively, our results indicate that ILA may positively regulate not only the expression of YAP and IL-22 but also the PI3K-AKT signaling pathways. Further research is required to fully elucidate its mechanisms of action.

Conclusions

In summary, we demonstrated a dysbiotic gut environment in the SBS piglets' models, characterized by a depletion of commensal microbial species, a decrease in beneficial microbes, and disruptions in the metabolism of indoles, carbohydrates, peptides, and benzoic acid. Multi-omics analysis suggested the decreased abundance of *Lactobacillus* may lead to a reduction in their metabolite ILA, which may affect intestinal proliferation and anti-inflammatory responses, thereby delaying the process of intestinal adaptation. Further study is needed to fully elucidate the underlying mechanisms. This study can help reveal a new therapeutic strategy for clinical practice and elucidate a novel mechanism of SBS. Future efforts to promote intestinal adaptation by supplementing the end products of microbiota may serve a high clinical efficacy.

Supplementary Information

The online version contains supplementary material available at https://doi.org/10.1186/s12986-025-00938-9.

Supplementary Material 1

Author contributions

Yongtao Xiao and Wei Cai: Conceptualization, methodology, project administrationand funding acquisition. Yongtao Xiao and Weipeng Wang: Designed the research, analyzed the data, wrote and revised the manuscript; Weipeng Wang, Ying Lu, Bo Wu, Shicheng Peng: Conduct the research and analyzed the data; All authors critically revised the manuscript, agree to be fully accountable for ensuring the integrity and accuracy of the work, and read and approved the final manuscript.

Funding

This work was supported by the National Natural Science Foundation of China (82470541, 82270537), Clinical Research Plan of SHDC (SHDC2020CR2010A), and Shanghai Science and Technology innovation Program (22Y31900600).

Data availability

No datasets were generated or analysed during the current study.

Declarations

Competing interests

The authors declare no competing interests.

Author details

[1]Department of Pediatric Surgery, Xin Hua Hospital, School of Medicine, Shanghai Jiao Tong University, No. 1665, Kong Jiang Road, Shanghai, China
[2]Division of Pediatric Gastroenterology and Nutrition, Xin Hua Hospital, School of Medicine, Shanghai Jiao Tong University, Shanghai, China
[3]Shanghai Institute of Pediatric Research, Shanghai, China
[4]Shanghai Key Laboratory of Pediatric Gastroenterology and Nutrition, Shanghai, China

Received: 6 February 2025 / Accepted: 5 May 2025
Published online: 22 May 2025

References

1. Caporilli C, Giannì G, Grassi F, Esposito S. An overview of Short-Bowel syndrome in pediatric patients: focus on clinical management and prevention of complications. Nutrients. 2023;15(10). https://doi.org/10.3390/nu15102341.
2. Radetic M, Kamel A, Lahey M, Brown M, Sharma A. Management of short bowel syndrome (SBS) and intestinal failure. Dig Dis Sci. 2023;68(1):29–37. https://doi.org/10.1007/s10620-022-07760-w.
3. Belza C, Wales PW. Management of pediatric intestinal failure related to short bowel syndrome. Semin Pediatr Surg. 2022;31(3):151175. https://doi.org/10.1016/j.sempedsurg.2022.151175.
4. Winkler M, Tappenden K. Epidemiology, survival, costs, and quality of life in adults with short bowel syndrome. Nutr Clin Practice: Official Publication Am Soc Parenter Enter Nutr. 2023;38(Suppl 1):S17–26. https://doi.org/10.1002/ncp.10964.
5. Phelps HM, Warner BW. Intestinal adaptation and rehabilitation. Semin Pediatr Surg. 2023;32(3):151314doi. https://doi.org/10.1016/j.sempedsurg.2023.151314.
6. Tappenden KA. Anatomical and physiological considerations in short bowel syndrome: emphasis on intestinal adaptation and the role of enterohormones. Nutr Clin Practice: Official Publication Am Soc Parenter Enter Nutr. 2023;38(Suppl 1):S27–34. https://doi.org/10.1002/ncp.10991.
7. Wang W, Wang Y, Lu Y, Tian X, Chen S, Wu B, et al. Inositol hexaphosphate promotes intestinal adaptation in short bowel syndrome via an HDAC3-mediated epigenetic pathway. Food Nutr Res. 2023;67. https://doi.org/10.29219/fnr.v67.8694.
8. Boutte HJ Jr., Chen J, Wylie TN, Wylie KM, Xie Y, Geisman M, et al. Fecal Microbiome and bile acid metabolome in adult short bowel syndrome. Am J Physiol Gastrointest Liver Physiol. 2022;322(1):G154–68. https://doi.org/10.1152/ajpgi.00091.2021.
9. Huang Y, Jiao J, Yao D, Guo F, Li Y. Altered fecal Microbiome and metabolome profiles in rat models of short bowel syndrome. Front Microbiol. 2023;14:1185463. https://doi.org/10.3389/fmicb.2023.1185463.
10. Budinska E, Gojda J, Heczkova M, Bratova M, Dankova H, Wohl P, et al. Microbiome and metabolome profiles associated with different types of short bowel syndrome: implications for treatment. JPEN J Parenter Enter Nutr. 2020;44(1):105–18. https://doi.org/10.1002/jpen.1595.
11. Pauline M, Fouhse J, Hinchliffe T. Probiotic treatment vs empiric oral antibiotics for managing dysbiosis in short bowel syndrome: impact on the mucosal and stool microbiota, short-chain fatty acids, and adaptation. 2022;46(8):1828–38.https://doi.org/10.1002/jpen.2377
12. Liu Y, Xiao Y, Chen S, Tian X, Wang W, Wang Y, et al. The farnesoid X receptor agonist tropifexor prevents liver damage in parenteral Nutrition-fed neonatal piglets. J Pediatr Gastroenterol Nutr. 2021;73(1):e11–9. https://doi.org/10.1097/mpg.0000000000003135.
13. Chen S, Xiao Y, Liu Y, Tian X, Wang W, Jiang L, et al. Fish oil-based lipid emulsion alleviates parenteral nutrition-associated liver diseases and intestinal injury in piglets. JPEN J Parenter Enter Nutr. 2022;46(3):709–20. https://doi.org/10.1002/jpen.2229.
14. Tsikis ST, Fligor SC, Hirsch TI, Mitchell PD, Pan A, Moskowitzova K, et al. A digestive cartridge reduces parenteral nutrition dependence and increases bowel growth in a piglet short bowel model. Ann Surg. 2023;278(4):e876–84. https://doi.org/10.1097/sla.0000000000005839.
15. Zhao J, Wan S, Sun N, Sun P, Sun Y, Khan A et al. Damage to intestinal barrier integrity in piglets caused by Porcine reproductive and respiratory syndrome virus infection. 2021;52(1):9310.1186/s13567-021-00965-3
16. Xiao Y, Zhou Y, Zhou K, Cai W. Targeted metabolomics reveals birth screening biomarkers for biliary Atresia in dried blood spots. J Proteome Res. 2022;21(3):721–6. https://doi.org/10.1021/acs.jproteome.1c00775.
17. Liang D, Liu Q, Zhou K, Jia W, Xie G, Chen T. IP4M: an integrated platform for mass spectrometry-based metabolomics data mining. BMC Bioinformatics. 2020;21(1):444. https://doi.org/10.1186/s12859-020-03786-x.

18. Babu M, Snyder M. Multi-Omics profiling for health. Mol Cell Proteom. 2023;22(6):100561doi. https://doi.org/10.1016/j.mcpro.2023.100561.
19. Wu H, Mu C, Xu L, Yu K, Shen L, Zhu W. Host-microbiota interaction in intestinal stem cell homeostasis. Gut Microbes. 2024;16(1):2353399. https://doi.org/10.1080/19490976.2024.2353399.
20. Boccia S, Torre I, Santarpia L, Iervolino C, Del Piano C, Puggina A, et al. Intestinal microbiota in adult patients with short bowel syndrome: preliminary results from a pilot study. Clin Nutr. 2017;36(6):1707–9. https://doi.org/10.1016/j.clnu.2016.09.028.
21. Cleminson JS, Thomas J, Stewart CJ, Campbell D, Gennery A, Embleton ND, et al. Gut microbiota and intestinal rehabilitation: a prospective childhood cohort longitudinal study of short bowel syndrome (the MIRACLS study): study protocol. BMJ Open Gastroenterol. 2024;11(1). https://doi.org/10.1136/bmjgast-2024-001450.
22. Zhang S, Nie Q, Sun Y, Zuo S, Chen C, Li S, et al. Bacteroides uniformis degrades β-glucan to promote Lactobacillus johnsonii improving indole-3-lactic acid levels in alleviating colitis. Microbiome. 2024;12(1):177. https://doi.org/10.1186/s40168-024-01896-9.
23. Wang W, Wang Y, Liu Y, Tian X, Chen S, Lu Y et al. Lactobacillus plantarum supplementation alleviates liver and intestinal injury in parenteral nutrition-fed piglets. 2022;46(8):1932–43.https://doi.org/10.1002/jpen.2429
24. Huang R, Wu F, Zhou Q, Wei W, Yue J, Xiao B, et al. Lactobacillus and intestinal diseases: mechanisms of action and clinical applications. Microbiol Res. 2022;260:127019doi. https://doi.org/10.1016/j.micres.2022.127019.
25. Fan Y, Pedersen O. Gut microbiota in human metabolic health and disease. 2021;19(1):55–71.https://doi.org/10.1038/s41579-020-0433-9
26. Wang G, Fan Y, Zhang G, Cai S, Ma Y, Yang L, et al. Microbiota-derived Indoles alleviate intestinal inflammation and modulate Microbiome by microbial cross-feeding. Microbiome. 2024;12(1):59. https://doi.org/10.1186/s40168-024-01750-y.
27. Wang A, Guan C, Wang T, Mu G. Lactobacillus-derived Indole derivatives ameliorate intestinal barrier damage in rat pups with complementary food administration. 2024;15(17):8775–87.https://doi.org/10.1039/d4fo02230k
28. Yu K, Li Q, Sun X, Peng X, Tang Q, Chu H et al. Bacterial indole-3-lactic acid affects epithelium-macrophage crosstalk to regulate intestinal homeostasis. 2023;120(45):e2309032120.https://doi.org/10.1073/pnas.2309032120
29. Xia Y, Liu C, Li R, Zheng M, Feng B, Gao J, et al. Lactobacillus-derived indole-3-lactic acid ameliorates colitis in cesarean-born offspring via activation of Aryl hydrocarbon receptor. iScience. 2023;26(11):108279doi. https://doi.org/10.1016/j.isci.2023.108279.
30. Laursen MF, Sakanaka M, von Burg N, Mörbe U. Bifidobacterium species associated with breastfeeding produce aromatic lactic acids in the infant gut. 2021;6(11):1367–82.https://doi.org/10.1038/s41564-021-00970-4
31. Ehrlich AM, Pacheco AR, Henrick BM, Taft D, Xu G, Huda MN et al. Indole-3-lactic acid associated with Bifidobacterium-dominated microbiota significantly decreases inflammation in intestinal epithelial cells. 2020;20(1):357.https://doi.org/10.1186/s12866-020-02023-y
32. Zhang FL, Chen XW, Wang YF, Hu Z, Zhang WJ, Zhou BW et al. Microbiota-derived Tryptophan metabolites indole-3-lactic acid is associated with intestinal ischemia/reperfusion injury via positive regulation of YAP and Nrf2. 2023;21(1):264.https://doi.org/10.1186/s12967-023-04109-3

Publisher's note